1 **Title: Accumulation of radiocarbon in ancient terrestrial landscapes: A small but significant**
2 **input of unknown origin**

3 **Authors:** Adrian Broz[1]*, Jerod Aguilar[2], Xiaomei Xu[3], and Lucas C.R. Silva[4,5]

4 **Affiliations:**

5 [1]Department of Earth Sciences, University of Oregon, Eugene, Oregon 97403

6 [2]Department of Earth Sciences, Southern Methodist University, Dallas, Texas 97403

7 [3]University of California Irvine, Irvine, California 92697

8 [4]Department of Geography, University of Oregon, Eugene, Oregon 97403

9 [5]Environmental Studies. Department of Biology. Institute of Ecology and Evolution, University of
10 Oregon, Eugene, Oregon 97403

11 *Corresponding author. Email: abroz@uoregon.edu

12
13 **Abstract:**

14 The persistence of soil organic carbon (C) in soil, defined as the mean residence time of organic C
15 compounds in soils, is a critical measure for understanding the capacity of terrestrial ecosystems to
16 regulate biogeochemical cycles. The persistence of organic carbon in soil is most often considered at
17 timescales ranging from tens to thousands of years, but the study of organic C in paleosols (i.e.,
18 ancient, buried soils) suggests that buried soils may have the capacity to preserve organic compounds
19 for tens of millions of years. A quantitative assessment of C sources and sinks from these ancient
20 terrestrial landscapes is complicated by additions of modern organic C, primarily due to the infiltration
21 of dissolved organic carbon. In this study, we quantify total organic C content and radiocarbon activity
22 in samples collected from 28- to 33-million-year-old paleosols that are naturally exposed as
23 unvegetated badland outcrops near eastern Oregon's "Painted Hills". The study site is part of a well-
24 mapped ~400-meter-thick sequence of Eocene-Oligocene (45-28 Ma) volcaniclastic paleosols, and
25 thus we expected to find "radiocarbon dead" samples preserved in deep layers of the lithified, brick-
26 like exposed outcrops. Total organic C, measured in three individual profiles spanning depth transects
27 from the outcrop surface to a 1-meter depth, range from 0.01 - 0.8 wt. % with no clear C-concentration
28 or age-depth profile. Ten radiocarbon dates from the same profiles reveal calibrated radiocarbon ages
29 of ~11,000 – 30,000 years BP that unexpectedly indicate additions of recent and /or modern organic C.
30 A two-endmember mixing model for radiocarbon activity suggests that modern C may compose ~0.5-
31 3.5% of the total organic carbon pool preserved in these ancient landscapes. We discuss several
32 mechanisms by which modern organic C could have infiltrated into the lithified, brick-like paleosol
33 surfaces and discuss potential implications for future research of ancient soils.

34

35

38

1. Introduction

40   The persistence of soil organic carbon (C), defined as the mean residence time of organic
41 compounds[1–3], is a key factor in determining whether soils function as C sources or C sinks[4]. Many
42 efforts to quantify soil C storage in modern soils are focused on temporal scales of tens to thousands
43 of years[5], but examination of organic matter preservation in paleosols (ancient, buried soils) suggests
44 that terrestrial environments may preserve organic matter over millions or even billions of years,
45 though at concentrations which are orders of magnitude lower than modern soils[6]. For example,
46 preserved organic carbon compounds in Archean (~2 Ga) paleosols include carbonaceous microfossils
47 and filamentous organic structures [7,8] which are thought to have originated from cyanobacterial mats
48 that lived on the soil surface[9]. Additionally, organic-walled fungal microfossils have been found in
49 Proterozoic (1 Ga) terrestrial environments[10]. Geologically younger paleosols contain pyrogenic
50 carbon[11,12], carbonaceous root traces[13,14], and carbonaceous compression fossils of plants that grew in
51 soils millions of years ago[15].
52   Critically, when buried soils are naturally exposed to the modern weathering zone, such as in
53 modern badlands that host sequences of paleosols, much of this ancient carbon can be oxidized by
54 modern biogeochemical processes and ultimately returned to the atmosphere[16]. The pool of ancient
55 carbon in exhumed terrestrial landscapes is not readily considered in terrestrial carbon budgets
56 because it is difficult to measure[16], and therefore quantifying the capacity of ancient soils to preserve
57 and/or cycle ancient organic carbon back to the atmosphere is not well constrained.
58   One challenge to a comprehensive understanding of long-term carbon storage in ancient
59 terrestrial landscapes is the widespread and pervasive additions of modern carbon from the modern
60 biosphere. This "contamination" by modern organic carbon can ultimately confound efforts to
61 understand organic matter persistence in ancient soils, in part because it is difficult to quantify the
62 sources and types of organic carbon in ancient terrestrial landscapes that are millions of years old. In
63 other words, additions of modern carbon to paleosols can inflate estimates of the so-called
64 "preserved" carbon. For example, carbon from microbial biomass and/or plant root exudates from the
65 modern weathering zone can leach downwards and accumulate in paleosols (e.g., [17]). Therefore, a
66 method to constrain the sources and approximate ages of organic carbon in bulk paleosol samples
67 would provide a valuable technique to understand if and how modern carbon accumulates in ancient
68 terrestrial landscapes.
69   In this work, we tested the hypothesis that unvegetated and highly lithified 28- to 33-million-
70 year-old paleosols contain small amounts of ancient radiocarbon-dead materials. We evaluated the
71 total carbon content of three lithified, brick-like paleosol profiles from eastern Oregon (Figure 1) and
72 performed radiocarbon analysis on bulk samples that were collected from the outcrop surface to a
73 horizontal depth of 1-meter into each outcrop. To quantify potential additions of modern organic
74 carbon as a function of horizontal depth into the outcrop, we employed a two-endmember isotopic
75 mixing model to estimate the percentage of modern carbon in ancient samples. Lastly, we used
76 thermal and evolved gas analysis to evaluate the thermodynamic stability of organic carbon in several
77 samples. We assessed evolutions of H_2O, CO_2 and organic fragments in bulk paleosol samples to
78 constrain whether organic compounds were primarily associated with clay minerals or other hydrated

79 phases. The objectives of this work were to A) determine whether 28 to 33-million-year-old paleosols
80 contain radiocarbon at depth; B) constrain the amount of modern carbon that could have
81 accumulated in ancient samples; and C) determine if organic carbon, whether ancient or modern, was
82 associated with clay minerals.
83
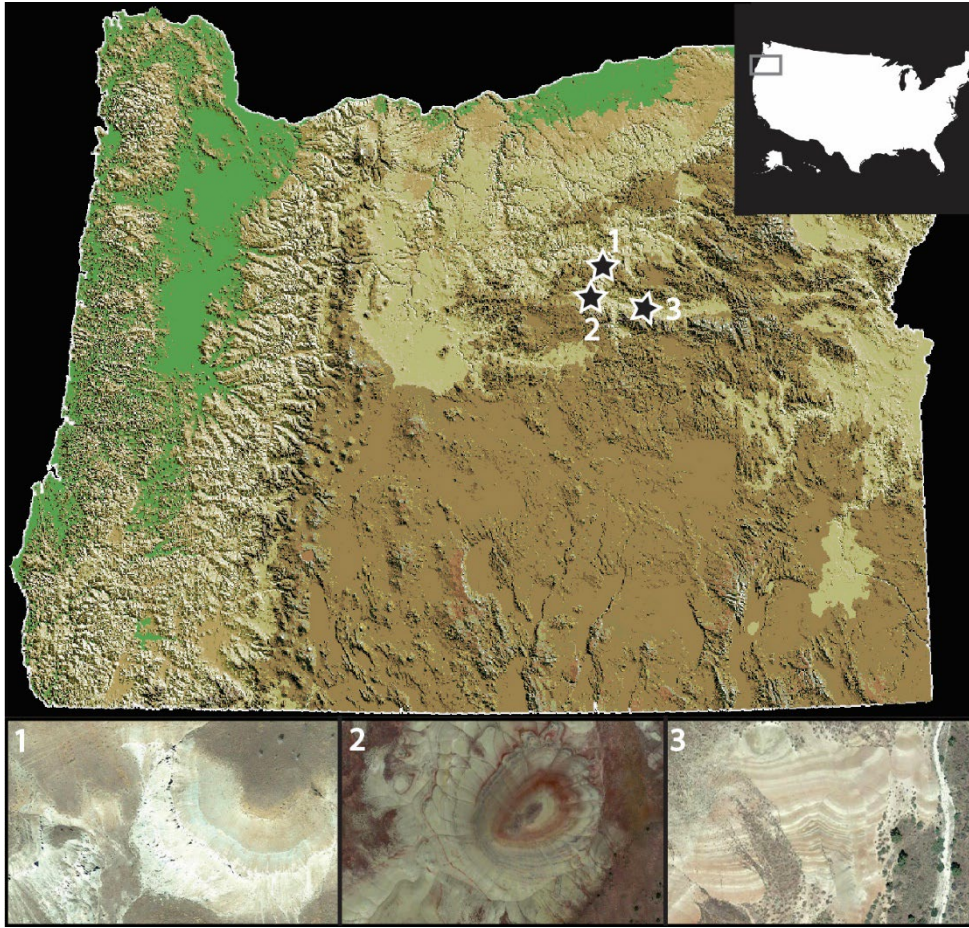
84

85 **Figure 1. Sampling sites from three ancient terrestrial landscapes near the John Day Fossil Beds**
86 **National Monument, eastern Oregon, USA. 1,** 28-million-year-old paleosols from the lower Turtle
87 Cove Member of the John Day Formation; **2** and **3**, 33-million-year-old paleosols from the middle Big
88 Basin member of the John Day Formation, near the local Eocene-Oligocene boundary (~33 Ma).

89   The eastern Oregon site has been previously considered as a "Mars-analog" site because the
90 mineralogy and geochemistry of the paleosol profiles resemble highly altered sedimentary rocks on
91 Mars that are approximately 3.7- 4.1 billion years old[18–20]. Past work at the Oregon site has examined
92 the mineralogy, diagenesis, and organic preservation potential of these ancient soils and their
93 pedogenic minerals for comparisons with Mars[20,21]. On Mars, putative paleosols contain pedogenic-like
94 minerals such as Al and Fe dioctahedral smectites, kaolins, hydrated silica, amorphous phases such as
95 allophane and/or imogolite, and hematite, which are altogether consistent with near-surface aqueous
96 alteration of mafic sediments under habitable conditions[22–24]. Importantly, these pedogenic minerals
97 may record information about the nature of climate and duration of aqueous activity on Mars, and
98 they may also be sites of enhanced organic preservation that could be targeted by current and future

99   Mars rovers. Similarly, many of the ~500 individual paleosol profiles at the Oregon field site contain
100   some, or all, of these minerals[15,20]. Most of the Oregon paleosol profiles formed as a result of sustained
101   pedogenic alteration of rhyodacitic to andesitic volcanic ash and tuff that was periodically emplaced
102   by nearby ancient stratovolcanoes from ~45-26 Ma[25]. However, the organic preservation potential of
103   these Mars-analog paleosols from Oregon is only partly understood. Previously, radiocarbon dating of
104   four samples collected from shallow depths (<40 cm) into a ~33 million year old paleosol outcrop
105   revealed a calibrated radiocarbon age of ~7,000-14,500 years BP, suggesting there had been inputs of
106   radiocarbon into the lithified, brick-like samples [21] (Table S1). This unanticipated finding motivated the
107   present work for radiocarbon dating of deeper samples across three additional profiles separated by
108   space and time.
109
110   **2. Methods**
111

Sample collection

113   Samples were collected from three paleosol outcrops within the Eocene-Oligocene (33-26 Ma)
114   John Day Formation in eastern Oregon (Figure 2). Two of the outcrops ("Luca" and "Lakim"), of an
115   estimated ~33 Ma, were in the middle Big Basin Member of the John Day Formation, and one ("Turtle
116   Cove"), of an estimated 28 Ma, was from the lower Turtle Cove Member of the John Day Formation[25].
117   Several measures were taken during sample collection to minimize organic contamination.
118   First, all sampling materials (glassware, foil, mortar and pestle) were ashed in a muffle furnace for 24 hr
119   at 550° C and wrapped in aluminum foil prior to arriving at the field site. All samples were collected in
120   glass vials and capped with aluminum foil prior to securing the plastic vial lids. An ashed sample of
121   silica sand served as a method-level blank and was carried through as many of the sampling steps as
122   possible. Nitrile gloves were worn during all stages of sample collection. Rock hammers and chisels
123   were flamed with isopropyl alcohol for 3-5 minutes prior to sample collection in order to ensure these
124   materials were sterile.
125   After removing the surface soil and exposing the lithified paleosol surface, rock hammers and
126   a chisel were used to trench to a depth of 100 cm at a horizontal angle into the outcrop. Large (~0.25
127   kg), lithified, brick-like samples were collected at depths of 0 cm (paleosol surface), 25 cm, 50 cm, 75
128   cm and 100 cm, wrapped in ashed aluminum foil, and immediately placed into a cooler for ~8 hours
129   before transport into a -80° C freezer.
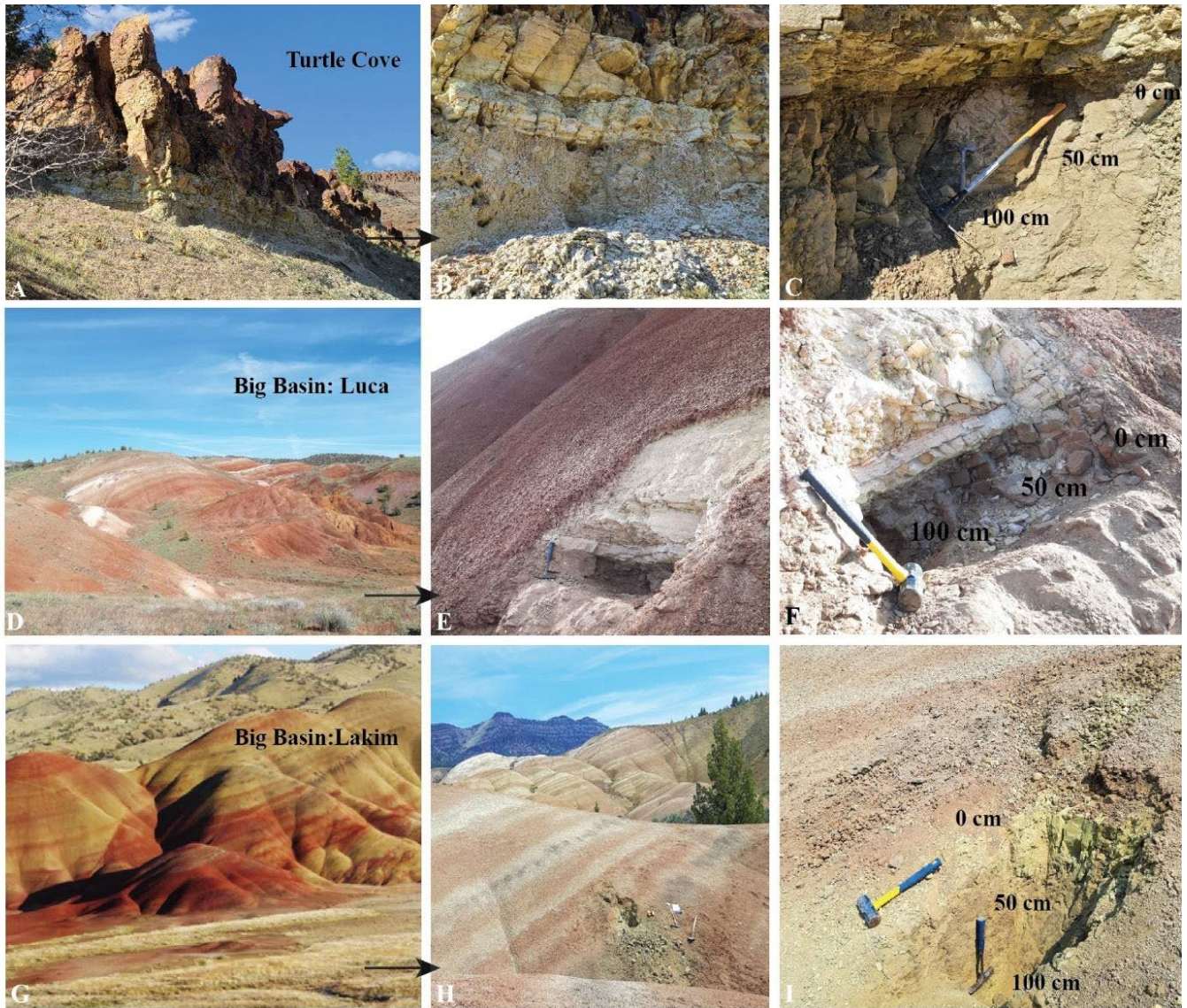
1

Figure 2. Ancient terrestrial outcrops sampled in this work. A), Oligocene (28 Ma) lower Turtle Cove Member of the John Day Formation (44.670229, -119.627418), and amorphous phase-rich Andisol paleosols buried by overlying ignimbrite (horizontal tan and brown layers); **B)** Early Oligocene (33 Ma) middle Big Basin Member of the John Day Formation (44.628605, -120.212263) and Al and Fe-smectite-rich Alfisol paleosol ("Luca" pedotype from[15]) buried by volcanic tuff (sharp white layer); **C)** Early Oligocene (33 Ma) middle Big Basin Member of the John Day Formation (44.638333, -120.220021) and Al/Fe smectite and Mn-oxide-bearing Inceptisol paleosol ("Lakim" pedotype from[15]) buried by gleyed biotite-bearing tuff (green layer)

Laboratory Analyses

Three independent laboratory analyses were performed to examine soil organic carbon (SOC) pools in the paleosol samples. First, we measured SOC abundances in bulk samples to determine if the samples contained sufficient quantities of organic carbon for radiocarbon dating. We then performed radiocarbon dating of bulk samples to identify any additions of recent/modern (radiocarbon) organic

145   carbon to the SOC pool. Third, we evaluated the thermal stability of SOC using thermal and evolved
146   gas analysis as a proxy for recalcitrance and dynamics of organic compounds in bulk samples[12,26]. By
147   monitoring evolutions of H_2O from phyllosilicate dehydroxylation and co-occurring releases of CO_2
148   and organic fragments from organic carbon decomposition, we determined if organic molecules were
149   associated with clay minerals and/or sulfate minerals in several of the samples.
150
151   **Total organic carbon determination and radiocarbon (^{14}C) dating**

152   All samples for total organic carbon determination and radiocarbon dating were acid-washed
153   to remove inorganic carbon. For acid washing, ground paleosol samples (~5 g) were treated with
154   approximately 20 mL of 0.1 M HCl at room temperature for 1 hour, washed three times with ~30 ml of
155   deionized water and then dried at 60° C for 24 hr. Samples were then manually encapsulated in 5×8
156   mm tin capsules (sample size approximately 0.25–0.70 mg). Total organic carbon was determined by
157   elemental analysis on a Costech ECS 4010 instrument at the University of Oregon with expected SD <
158   0.3%[27]. The TOC in each sample was calculated to optimize aliquot amounts for radiocarbon dating. All
159   samples were analyzed in duplicate.
160   Radiocarbon dating of modern soil samples is a proxy for mean soil organic carbon age[28] and
161   was used here to determine if paleosols contain radiocarbon at depth. A radiocarbon age of organic
162   carbon was obtained from ten samples across three paleosol profiles. Radiocarbon dating of acid-
163   washed paleosol samples was performed at the W.M. Keck Carbon Cycle Accelerator Mass
164   Spectrometer at the University of California, Irvine. An additional TOC determination of these samples
165   prior to radiocarbon dating was performed at UC Irvine and is reported in Table 2. The accuracy and
166   precision (1 σ) of this analysis on modern carbon ($\Delta^{14}C$ >0‰) was better than 9‰. Laboratory blanks
167   yielded a $\Delta^{14}C$ value of -996.2 ‰.
168
169   **Quantifying additions of modern carbon to bulk paleosol samples**

170   To test the hypothesis that paleosols contained modern organic carbon, we used an isotopic
171   mixing model to estimate the relative proportion of modern carbon in bulk paleosol samples. Based
172   on the distinct isotopic composition of modern organic carbon and radiocarbon-free Oligocene
173   carbon, a two-endmember mixing model[29,30] was used to quantify the relative proportions of modern
174   and ancient carbon as distinct sources of the paleosol organic carbon pool[17]. We used the following
175   equation to partition modern (post-bomb) organic carbon ($D^{14}C = 0$ ‰) from radiocarbon-dead
176   Oligocene organic carbon ($D^{14}C \sim -999$‰):

177    $$C_{modern} = C_t(D^{14}C_{bulk} - D^{14}C_{Oligocene})/(D^{14}C_{Modern} - D^{14}C_{Oligocene}) \qquad (1)$$

178   Where C_t is the total amount of organic carbon (TOC) measured in bulk samples, $D^{14}C_{bulk}$ is the
179   measured $D^{14}C$ value of bulk samples, $D^{14}C_{Modern}$ is a typical value for a modern organic carbon
180   endmember ($D^{14}C = 0$‰), $D^{14}C_{Oligocene}$ is a typical $D^{14}C$ value for a radiocarbon-free organic carbon
181   endmember ($D^{14}C =$ approximately -999‰), and C_{modern} is the modelled fraction of modern organic
182   carbon in bulk samples. Errors were propagated to estimate uncertainty associated with modelled
183   values. The sources of uncertainty considered in the model were a) the uncertainty of the measured
184   TOC values and b) uncertainty of the measured $D^{14}C$ values.

185 **Thermal and Evolved Gas Analysis**

186   We used thermal and evolved gas analysis to examine two out of the ten samples that were
187 radiocarbon dated. Thermal and evolved gas analysis is an analytical technique that allows for
188 characterizing the organic and mineral content of natural soil and sediment samples[31]. Ramped
189 combustion from 35° C – 1000° C generates a time and temperature curve for each volatile gas (e.g.,
190 CO_2, H_2O, SO_2) released during the thermal decomposition of the sample. This technique constrains
191 the amount and thermodynamic stability of organic carbon in bulk samples[32], as well as identifying if
192 organic carbon was associated with phyllosilicates or other volatile-bearing minerals[33,34]. The peak
193 release temperature of CO_2 from organic carbon decomposition can also reveal differences in the
194 thermodynamic stability of organic carbon compounds in the SOC pool[35]. Because there are large
195 differences in the thermal stability of labile and recalcitrant organic carbon compounds [31,36] it is
196 possible to constrain the thermodynamic stability (e.g., resistance to oxidation) of organic carbon in
197 bulk paleosol samples. This can be used to help evaluate whether paleosol samples contain significant
198 amounts of labile modern organic carbon that could have originated in the modern weathering zone.
199   A Setaram Labsys Evo differential scanning calorimeter (DSC)/thermal gravimeter (TG)
200 connected to a Pfeiffer Omnistar quadrupole mass spectrometer (QMS) at NASA Johnson Space
201 Center was used for thermal and evolved gas analysis. Approximately 50 mg ± 3 mg of ground
202 paleosol sample was placed in an Al_2O_3 sample crucible (previously ashed at 550° C before
203 introduction of the sample). The sample crucible and an identical empty reference crucible were
204 placed in the furnace. The instrument was then purged twice with helium to remove any
205 contamination in the system, then set to a pressure of 3 kPa He prior to sample analyses. Helium was
206 chosen as a carrier gas because it is inert. Samples for EGA were not acid-washed before analysis.
207 Ramped EGA takes advantage of the large differences in thermal stability of organic and inorganic
208 carbon to simultaneously examine both carbon pools in bulk soil samples without acid
209 pretreatment[32]. The crucibles containing samples were heated from approximately 35 °C to 1000 °C at
210 a heating rate (ramp rate) of 35°C/min and with a helium flow rate of 10 cm^3/s. A series of three blanks
211 were analyzed before and after each group (n=10) of samples. Volatiles ranging from mass/charge
212 (*m/z*) 1 - 100 were measured. All analyses were performed in duplicate. All sample runs were
213 background corrected.
214

3. Results and Discussion

216   Total organic C, measured in three individual profiles spanning depth transects from the outcrop
217 surface to a 1-meter depth, range from 0.01 - 0.8 wt. % with no clear C-concentration or age-depth
218 profile (Table 1). Radiocarbon dating of 10 samples from three different paleosol profiles showed raw
219 $D^{14}C$ values ranging from -768.3 ‰ ± 1.3‰ to -971.9‰ ± 0.9‰ and calibrated ages between 11,750 ±
220 50 years BP and 30,110 ± 320 years BP (Table 1). All samples contained radiocarbon. The fraction of
221 modern carbon (FM) ranged from 0.0236 ± 0.008 to 0.2333 ± 0.013 (Table 1) and was highest in the
222 Luca profile and lowest in the Turtle Cove profile (Figure 2). One of the pedotypes (Luca) is a highly
223 oxidized paleosol with very low TOC; thus, only one sample from this profile was able to be
224 radiocarbon-dated, and this sample required combustion of over 1 g of material **(Table S2)**.

225

Table 1. Total organic carbon and radiocarbon analysis of ten paleosol samples from eastern Oregon. Depth (cm) represents the horizontal depth into the outcrop from where samples were gathered. TOC, total organic carbon, measured at University of Oregon; FM, fraction of modern; Ma, Millions of years ago. The estimated age of the outcrop ("Age") was previously determined by [40]Ar-[39]Ar dating (Bestland, 1997) and is distinct from ^{14}C age (years BP).

231

Sample	Depth (cm)	Age	TOC (wt. %)	Fraction modern	Error ±	D[14]C	Error ±	[14]C age (Yrs BP)	Error ± (Yrs)
Lakim	0	~33 Ma	0.302	0.0570	0.0009	-943.0	0.9	23020	130
Lakim	25	~33 Ma	0.116	0.1358	0.0010	-864.2	1.0	16040	70
Lakim	50	~33 Ma	0.128	0.0795	0.0009	-920.5	0.9	20340	90
Lakim	75	~33 Ma	0.251	0.0547	0.0009	-945.3	0.9	23340	140
Lakim	100	~33 Ma	0.132	0.1808	0.0012	-819.2	1.2	13740	60
Luca	0	~33 Ma	0.060						
Luca	22	~33 Ma	0.014	0.2317	0.013	-768.3	1.3	11750	50
Luca	50	~33 Ma	0.005						
Luca	75	~33 Ma	ND[℧]						
Luca	100	~33 Ma	0.001						
TC	0	~28 Ma	0.170	0.0281	0.0013	-971.9	0.9	28700	260
TC	25	~28 Ma	0.196	0.0285	0.0009	-971.5	0.8	28590	230
TC	50	~28 Ma	0.261	0.0236	0.0008	-976.4	0.9	30110	320
TC	100	~28 Ma	0.115	0.0621	0.0009	-937.9	0.9	22330	120

[℧] ND = No detection; below limit of quantification

232

233   Two hypotheses to explain the calibrated radiocarbon dates are A) additions of modern organic
234 carbon to bulk samples (e.g., a D[14]C ~ 0‰ modern carbon pool mixing with an ancient, radiocarbon-
235 free pool); or B) a Pleistocene (~11-30 Ka) productivity event which introduced carbon into the
236 paleosols (e.g., the carbon is indeed tens of thousands of years old).
237   One possible source of radiocarbon may derive from precipitation-driven leaching of dissolved
238 organic carbon from modern biota living in the current weathering zone above the paleosol outcrop.
239 As such, it is possible that small amounts of modern organic carbon from the weathered zone above
240 paleosol outcrops have mixed with larger amounts of ^{14}C-free organic carbon that is endogenous (e.g.,
241 autochthonous) to paleosols. In this way, a radiocarbon date of ~11,000-30,000 years BP could
242 represent a mixing of modern organic carbon and 33 Ma organic carbon. This hypothesis is supported
243 by the erosion rate for the site, which was previously determined to be approximately 4.94 ± 0.05
244 mm/year[37]. Using this erosion rate, the ~20 cm-thick soils that formed on top of the paleosol outcrops
245 are only about 40 years old and could have leached modern organics into the underlying paleosols
246 during this time.
247   Application of a two-endmember isotopic mixing model to the measured D[14]C values (Equation 1)
248 for estimation of modern organic carbon abundances in bulk paleosol samples is shown in Table 2.

249 The modelled abundances of modern carbon ranged from 0.46 ± 0.02 % to 2.36 ± 0.03 % of the total
250 organic carbon in each sample. These results support the hypothesis that the measured $D^{14}C$ values
251 represent the mixing of small amounts of modern organic carbon with larger amounts of radiocarbon-
252 free Oligocene carbon.
253
254 **Table 2. Application of a two-endmember mixing model to the measured $D^{14}C$ values in ten**
255 **paleosol samples.** TOC – Total organic carbon, measured at UC Irvine; FM, Fraction modern; Modern
256 C, modelled abundance of modern carbon in bulk paleosol samples, representing the percent modern
257 carbon of the measured TOC of bulk samples.

Paleosol	Depth (cm)	TOC (wt. %)	TOC ±	1/TOC	FM	$D^{14}C$ (‰)	$D^{14}C$ ± (‰)	Modern C (%)	Error (%)
Lakim	0	0.26	0.001	3.80	0.057	-943.05	0.9	1.47	0.004
Lakim	25	0.09	0.001	11.21	0.136	-864.23	1.0	1.20	0.011
Lakim	50	0.14	0.001	7.07	0.080	-920.46	0.9	1.11	0.007
Lakim	75	0.24	0.001	4.23	0.055	-945.29	0.9	1.27	0.004
Lakim	100	0.03	0.001	30.86	0.181	-819.15	1.2	2.36	0.031
Luca	22	0.01	0.003	71.43	0.232	-768.34	1.30	0.58	0.183
TC	0	0.17	0.004	5.87	0.028	-971.94	0.9	0.46	0.021
TC	25	0.15	0.004	6.80	0.028	-971.55	0.8	0.54	0.026
TC	50	0.23	0.008	4.35	0.024	-976.44	0.9	0.59	0.033
TC	100	0.08	0.032	11.82	0.062	-937.92	0.9	0.70	0.373

258

Constraining the ^{14}C signal of old carbon in bulk paleosol samples

260 To test the hypothesis that mixing of modern and Oligocene carbon caused the measured
261 radiocarbon ages, we took a Keeling plot approach[38] to estimate the ^{14}C signal of the old-carbon
262 endmember in paleosols. We performed least-squares regressions of the fraction modern (FM) versus
263 1/TOC and considered the intercept as the FM of the old-carbon endmember[38]. Figure 3A shows the
264 positive significant relationship between FM and 1/TOC in two of the paleosol profiles. The modelled
265 FM of the old-carbon endmember in the Lakim profile was 0.047 ± 0.0012. By contrast, the Turtle Cove
266 profile had an intercept of 0.004 ± 0.0012, which was consistent with a near radiocarbon-dead sample,
267 suggesting this sample contained primarily Oligocene carbon.

268 The modelled FM values agree with the modelled abundances of modern carbon in each of
269 the paleosol profiles (Table 1), e.g., the profile with the greatest modelled amount of modern carbon
270 (Lakim) also had the highest FM, while the profile with the least amount of modern carbon (Turtle
271 Cove) had a much older ^{14}C signature for the old-carbon endmember, and thus a lower FM (Figure 3B).
272 Interestingly, this sample also had the highest TOC (0.8 wt. %), which suggests this paleosol contains
273 large amounts of predominantly Oligocene carbon. This also constitutes a major result because it
274 suggests that paleosols rich in amorphous phases and phyllosilicates, such as the Turtle Cove sample,
275 can preserve soil organic carbon over geological timescales. Altogether, these results support the
276 hypothesis that the measured radiocarbon dates represent a mixing of modern and ancient carbon in
277 bulk paleosol samples and demonstrate the heterogeny of radiocarbon accumulation across ancient
278 terrestrial landscapes.

279
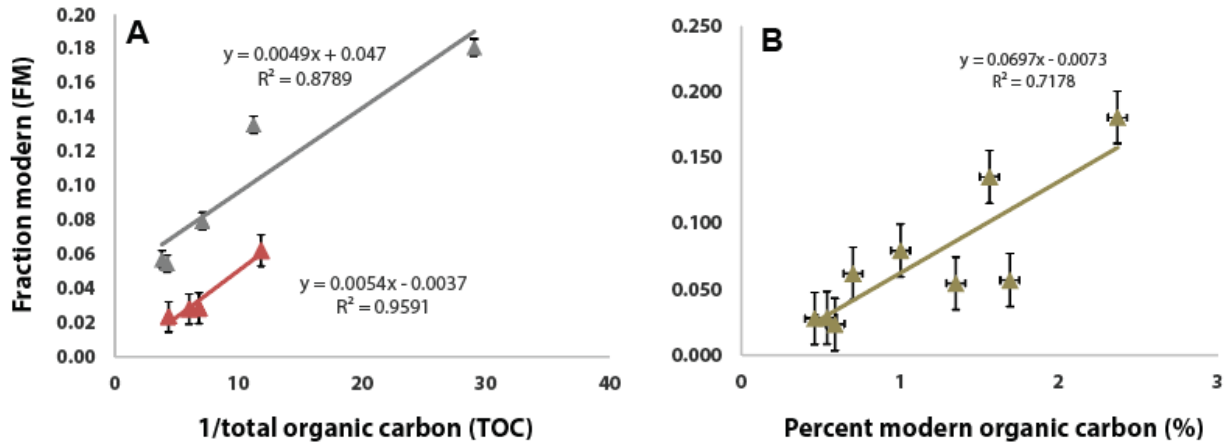
Figure 3. Application of a two-endmember isotopic mixing model to measured D^{14}C values of bulk paleosol samples. A) application of a Keeling plot approach to estimate the ^{14}C signal of the old-carbon endmember of two paleosol profiles, where the ^{14}C signal is the y-intercept in each of the two equations; B) the relationship between fraction modern (FM) values from bulk samples and the modelled abundance of modern organic carbon

Figure 4 demonstrates the nature of radiocarbon accumulation in two paleosol profiles as a function of horizontal depth into the exposed outcrop. One striking observation in the Turtle Cove soil was the significant (P <0.001) relationship between horizontal depth into the outcrop and the percent of modern carbon (n=4; R^2 = 0.9939). However, it should be noted that there were only four data points considered for the Turtle Cove soil, and thus these results should be interpreted with caution due to the low sample size. The Lakim soil showed a more erratic depth function (Figure 3B), likely because the 50 cm and 75 cm samples contained significantly (P<0.05) less modern organic carbon than most other samples in the transect. Interestingly, the deepest samples in the two profiles (100 cm) contained the highest modelled abundances of modern organic carbon.

294

295
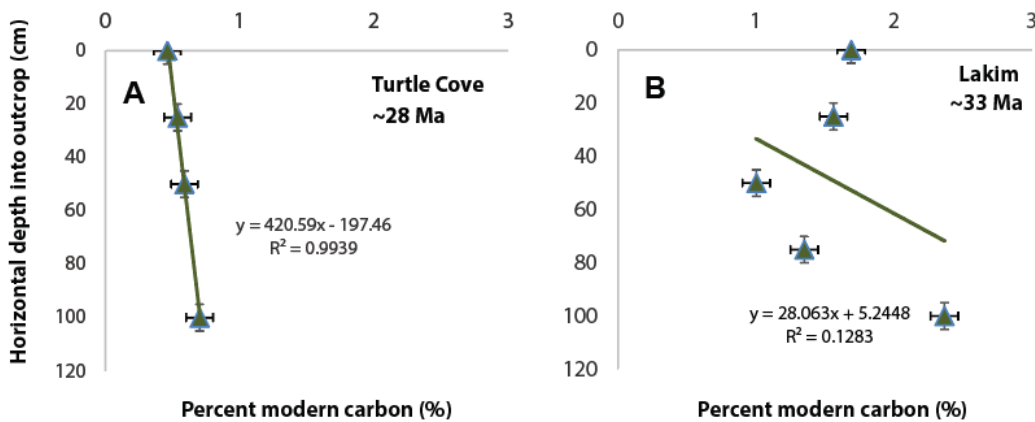
Figure 4. The relationship between sampling depth and the modelled percent of modern carbon in two Oligocene (28-33 Ma) paleosol profiles

298

299   Although it is challenging to determine what specific biogeochemical processes may have led
300   to the depth functions, differences in topography and the resulting sampling protocol between the
301   soils could explain the relationship between depth and modern carbon abundance (Figure 4). The
302   Lakim soil was trenched at a ~65° angle relative to the surface due to the gentle sloping nature of the
303   outcrop (slope ~45°), whereas the Turtle Cove sample was trenched at a nearly horizontal ~90° angle
304   relative to the surface because the outcrop was a near-vertical wall (slope ~90°) (Figure 2). This could
305   have ultimately led to the observed radiocarbon trends in each of the soils. Alternatively, the
306   precipitation-driven leaching of dissolved organic carbon could have infiltrated deep (> 1 m) into the
307   matrix of the exhumed paleosols in an inherently heterogenous manner, such as along randomly
308   oriented fractures in the lithified matrix.

309   Topography could have further influenced the leaching of dissolved modern organic carbon
310   because of differences in permeability of overlying materials. The Turtle Cove outcrop was buried by
311   several ash layers and then a relatively impermeable ignimbrite (Figure 2) whereas the Lakim and Luca
312   soils were buried by a biotite-bearing tuff, which presumably has higher permeability compared to the
313   ignimbrite. An additional possibility is widespread groundwater-driven accumulation of dissolved
314   organic carbon, but there was no morphological evidence of modern groundwater alteration in any of
315   the profiles examined.

316   On the other hand, it is possible that Pleistocene-age carbon could have accumulated in the
317   soils, possibly from leaching of dissolved organic carbon resulting from a Pleistocene (11-30 Ka)
318   productivity event. Previous work has shown that the field site was ice-free and adjacent to pluvial
319   lakes during the late Pleistocene[39]. Other work has shown that eastern Oregon was characterized by
320   highly productive pluvial lakes and grassland soils associated with Pleistocene Megafauna (e.g.,
321   "Mammoth Steppe")[40]. Therefore, it is possible that organic carbon from the weathering zone leached
322   into paleosols at that time.

323   **Thermal and evolved gas analysis (EGA)**

324   Thermal analysis techniques have been employed for understanding the nature and stability
325   of organic matter in modern terrestrial soils, though at present there are limited studies of paleosols.
326   While pyrolysis EGA does not provide insight into the specific types of organic compounds present, it
327   can provide information about the thermodynamic stability of organic carbon[26,35], and whether
328   organic compounds are associated with minerals such as phyllosilicates and sulfates[33]. Since paleosols
329   are known to preserve endogenous organic carbon in association with clay mineral surfaces over
330   hundreds of millions of years [9,41], it is important to determine if the Oregon paleosols contain organic
331   carbon, whether ancient or modern, that is associated with clay minerals or other volatile-bearing
332   phases. Many of the paleosols examined in the present study contained between ~70-95 wt. % Al and
333   Fe smectites, primarily as mixtures of montmorillonite and nontronite[20]. Therefore, thermal analysis of
334   bulk samples and their inherently high clay content could help to constrain if organic molecules are
335   present in association with clay minerals.

336   Additional minerals may also have contributed to organic preservation in paleosols. Past work
337   determined that several of the samples analyzed here contained trace amounts of sulfate minerals
338   (gypsum and jarosite) that were likely inherited from the modern weathering zone and not original to
339   the paleosol [20]. During EGA, simultaneous releases of SO_2 and CO_2 would indicate that organics,

340   whether ancient or modern, could have also been associated with sulfate minerals (e.g., sorbed or
341   occluded), or preserved as organo-sulfur compounds through abiotic reactions such as sulfurization of
342   organic matter [42–44].
343   Figure 5 shows the thermal and evolved gas analysis (EGA) of two paleosol samples. The DSC
344   and volatile curves were representative of a complex pedogenic mineral matrix, with many different
345   exothermic and endothermic reactions simultaneously occurring over a range of temperatures. In
346   general, CO_2 and organic fragments from organic carbon decomposition had a consistent peak release
347   temperature at ~400° C which tracked with a small exotherm, suggesting the presence of recalcitrant
348   organic carbon with resistance to low-temperature (150- 300° C) oxidation (Figure 5). On the other
349   hand, high-temperature (> 550° C) evolutions of CO_2 in paleosol samples (Figure 5) which tracked with
350   an endotherm were instead consistent with the thermal decomposition of inorganic carbon (e.g.,
351   small amounts of carbonate) and were not characteristic of organic carbon decomposition.
352   Samples for EGA were not acid washed (see Methods) because acid pretreatment steps to
353   remove carbonates have been shown to alter original quantities of TOC in samples[32]. Thus, it is
354   possible that small amounts of carbonates were present in our samples. However, soil organic matter
355   that is associated with clay minerals can also have CO_2 release temperatures that overlaps with the
356   CO_2 release from inorganic carbon in the ~550-700° C range[32,34], primarily because interactions with
357   mineral surfaces can increase the thermodynamic stability of organic carbon, which can lead to an
358   increase in the temperature of thermal decomposition during pyrolysis [26]. For example, mineral-
359   associated organic carbon could have been responsible for the high temperature (~700° C)
360   exothermic CO_2 peaks observed in both samples (Figure 5, red trace). Alternatively, this CO_2 peak could
361   have resulted from the thermal decomposition of refractory organic carbon such as kerogen [33], or from
362   the decomposition of inorganic C. Since these ancient soils were at one point buried by an estimated
363   1-2 km of overburden[15], refractory organic compounds could have formed as a result of burial and
364   diagenesis[6].
365
366
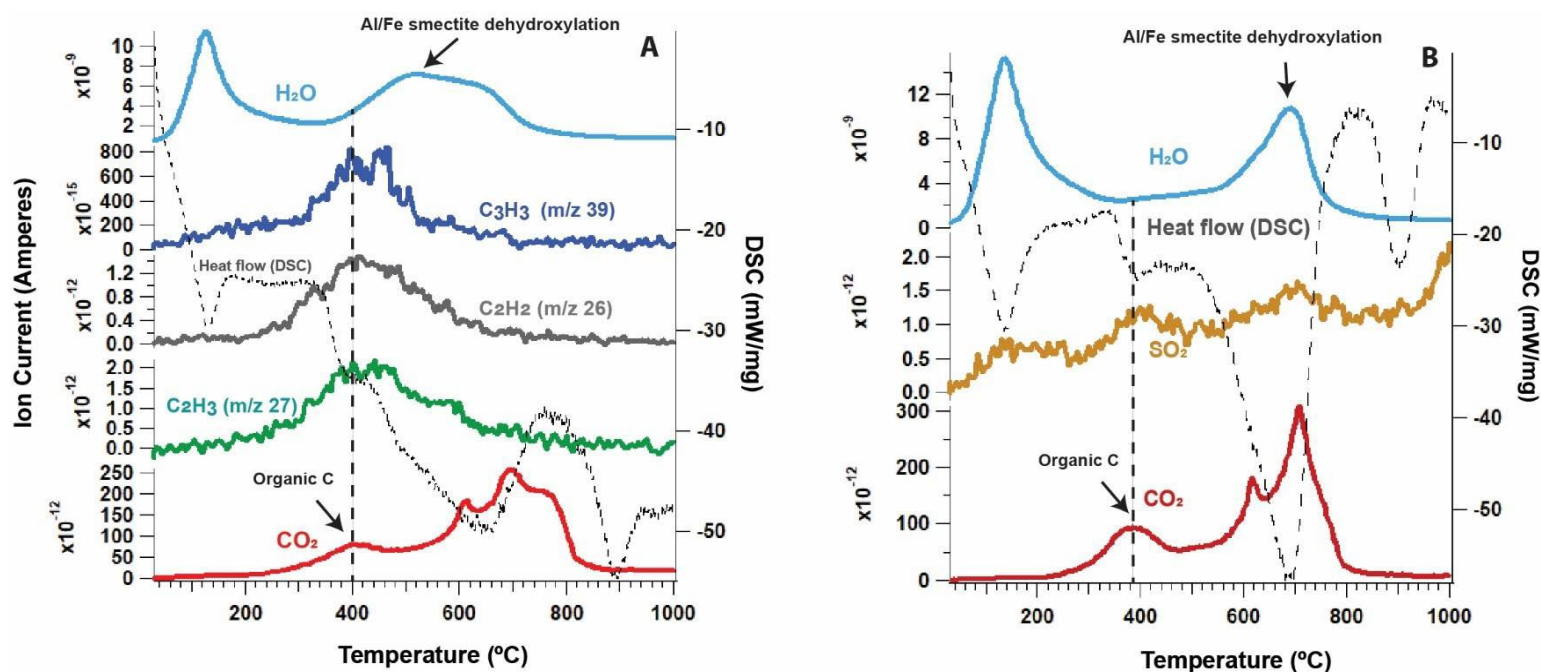
Figure 5. Thermal and evolved gas analysis of two paleosol samples from the early Oligocene (33 Ma) Big Basin Member of the John Day Formation. **A),** Evolutions of CO_2, organic fragments (C_2H_2, C_2H_3, C_3H_3), and H_2O from the surface horizon of the Luca paleosol. Dashed trace is heat flow from differential scanning calorimetry (DSC) where exothermic reactions have a positive slope; **B)** Evolutions of H_2O (blue trace), SO_2 (yellow trace), CO_2 (red trace), from a thin Entisol stratigraphically below the Luca profile (adapted from [21]). Dashed vertical line at 400° C in both panels is from the thermal decomposition of organic carbon. H_2O – m/z 18, SO_2 – m/z 64, CO_2 – m/z 44

In our samples, there was no clear EGA evidence that organic carbon was predominantly associated with clay minerals (e.g., chemisorbed) because the peak release temperature of CO_2 and organic fragments from organic carbon decomposition at 400° (vertical dotted lines, Figure 5) was offset by approximately 100° C from the peak H_2O release from phyllosilicate dehydroxylation (~500-650° C). If organic molecules were strongly associated with clay mineral surfaces and/or interlayers, there would be little or no apparent offset between CO_2 and H_2O (e.g., the two peaks would present as co-evolving). Similar CO_2 peak release temperatures of 400 – 500° C were noted by other authors in the Pleistocene "Brady" paleosol from Nebraska, which was attributed to the preservation of highly recalcitrant organic carbon such as black carbon (char) and plant lipids[12]. Additionally, we observed small amounts of evolved SO_2 that overlapped with organic carbon decomposition at ~400° C (yellow trace, Figure 5b), suggesting the presence of organo-sulfur compounds[45] or the decomposition of a sulfide mineral[46]. Thus, sulfur-bearing phases could have also contributed to the preservation of ancient or modern organic carbon.

Though the EGA results do not provide direct evidence that phyllosilicates and organics were strongly associated with one another, it is possible that the high clay mineral abundances provided other means of organic preservation, including physical occlusion, the formation of organic-mineral aggregates, or other weaker types of sorption to phyllosilicate surfaces, such as outer-sphere complexation[47,48] which could have resulted in the organic carbon decomposing at temperatures

393 ~100-200° C lower than clay mineral dehydroxylation. Physical soil fractionation to concentrate clay
394 minerals and associated organics may provide more useful results than EGA of bulk samples as
395 performed here, though may prove challenging because of the lithification and diagenetic alteration
396 that have acted upon ancient soil samples. In any case, an evaluation of mineral-associated organic
397 carbon content using conventional methods (e.g.,[12]) would be useful to confirm the EGA results
398 presented here. These results illustrate the complexity of the organic carbon pool within ancient,
399 buried soils, and they also demonstrate the fundamental limitations of pyrolysis methods such as EGA
400 for constraining the organic and inorganic C content of these materials.
401

402 **4. Conclusion**

403   The objectives of this work were to A) determine whether 28 to 33-million-year-old paleosols
404 contain radiocarbon at depth; B) constrain the amount of modern carbon that could have
405 accumulated in ancient samples; and C) determine if organic carbon, whether ancient or modern, was
406 predominantly associated with clay minerals. Radiocarbon analysis of 10 samples collected from three
407 different naturally exhumed paleosol profiles separated by time and space showed widespread
408 accumulation of radiocarbon. The total organic carbon content of bulk samples ranged from 0.01 $\pm$
409 0.003 wt. % to 0.26 $\pm$ 0.001 wt. %. The measured $D^{14}C$ values ranged from -768.3 ‰ $\pm$ 1.3‰ to -
410 971.9‰ $\pm$ 0.9‰ and calibrated radiocarbon ages ranged between 11,750 $\pm$ 50 years BP and 30,110 $\pm$
411 320 years BP. The fraction of modern carbon (FM) ranged from 0.0236 $\pm$ 0.008 to 0.2333 $\pm$ 0.013. There
412 was no apparent radiocarbon age-depth relationship in any of the profiles, suggesting heterogenous
413 and erratic accumulation of radiocarbon within the lithified, brick-like paleosol samples.
414   Application of a two-endmember isotopic mixing model based on measured $D^{14}C$ values of
415 bulk samples suggested that modern organic carbon comprised approximately 0.46 $\pm$ 0.02 % to 2.36 $\pm$
416 0.03 % of the paleosol total organic carbon pool. A Keeling plot approach to determine the ^{14}C
417 signature of the old-carbon endmember in paleosols also suggested a mixing of modern carbon and
418 potentially Oligocene (radiocarbon-free) carbon. The modelled FM of the old-carbon endmember in
419 two paleosol profiles ranged from 0.004 $\pm$ 0.0012 to 0.047 $\pm$ 0.0012, both of which are consistent with
420 a near radiocarbon-dead old-carbon endmember.
421   Thermal and evolved gas analysis was used to constrain the thermodynamic stability of
422 organic carbon and to determine if organic carbon was primarily associated with clay minerals. A CO_2
423 peak release temperature at 400° C that co-occurred with evolutions of organic fragments was
424 consistent with the presence of recalcitrant organic carbon. There was no direct evidence that organic
425 carbon, whether ancient or modern, was strongly associated with phyllosilicates (e.g., chemisorbed)
426 because the peak release temperature of CO_2 (from organic carbon decomposition) and H_2O release
427 (from smectite dehydroxylation) were offset by ~100-200° C. Altogether, these results support the
428 hypothesis that the measured Pleistocene radiocarbon dates (~11-30 Ka) most likely represent a
429 mixing of small quantities of modern organic carbon from the current weathering zone, which has
430 mixed with larger amounts of radiocarbon-free paleosol organic carbon that may have been
431 preserved for millions of years. Although the sources and types of organic compounds remain
432 unexplored, this work reveals the widespread accumulation of radiocarbon in lithified, brick-like
433 paleosols that are millions of years old and suggests the accumulation of radiocarbon may be a

434 common process within ancient, exhumed terrestrial landscapes. Ultimately, results from this work
435 cannot elucidate the mechanisms nor the sources of radiocarbon activity in these landscapes but
436 instead highlight the erratic nature of radiocarbon accumulation in rapidly eroding ancient terrestrial
437 landscapes.

438
439

440 **Additional Information**

441

442 **Acknowledgements**

449

450 **Author Contribution Statement**

451 A.P.B and J.A designed the study, conducted fieldwork, performed laboratory analyses and
452 drafted the manuscript. X.X. performed radiocarbon dating and conducted data analysis and
453 interpretation. L.C.R.S conceived the study and supervised the project. All authors contributed to the
454 manuscript.

455

456 **Author Disclosure Statement**

457 No competing financial interests exist.

458

459 **Data Availability Statement**

460 All data supporting the conclusions can be found within the article and in the
461 following repository: Broz, 2022. All raw data to reproduce EGA traces are included in the
462 supplementary dataset (Broz, 2022).

463

464 ## 5. References

465

466 Apesteguia, M., Plante, A.F., and Virto, I., 2018, Methods assessment for organic and
467   inorganic carbon quantification in calcareous soils of the Mediterranean region:
468   Geoderma Regional, v. 12, p. 39–48, doi:10.1016/j.geodrs.2017.12.001.
469 Bestland, E.., 1997, Alluvial Terraces and Paleosols As Indicators Of Early Oligocene Climate
470   Change (John-Day Formation, Oregon): Journal Of Sedimentary Research, v. 67, p. 840–
471   855, doi:10.1306/D4268653-2B26-11D7-8648000102C1865D.
472 Bishop, J.L., Fairén, A.G., Michalski, J.R., Gago-duport, L., Baker, L.L., Velbel, M.A., Gross, C.,
473   and Rampe, E.B., 2018, Surface clay formation during short-term warmer and wetter

474   conditions on a largely cold ancient Mars: Nature Astronomy, v. 2, p. 206–213,
475   doi:10.1038/s41550-017-0377-9.
476 Bossio, D.A. et al., 2020, The role of soil carbon in natural climate solutions: Nature
477   Sustainability, doi:10.1038/s41893-020-0491-z.
478 Broz, A.P., 2020, Organic Matter Preservation in Ancient Soils of Earth and Mars: Life, v. 10,
479   doi:doi:10.3390/life10070113.
480 Broz, A.P., Clark, J., Sutter, B., Ming, D.W., Horgan, B., Douglas, P., Jr, A., and Silva, L.C.R.,
481   2022a, Detection of organic carbon in Mars-analog paleosols with thermal and evolved
482   gas analysis: Journal of Geophysical Research: Planets (in revision),
483   doi:https://doi.org/10.31223/X50G88.
484 Broz, A.P., Clark, J., Sutter, B., Ming, D.W., Tu, V., Horgan, B., and Silva, L.C.R., 2022b,
485   Mineralogy and diagenesis of Mars-analog paleosols from eastern Oregon, USA:
486   Icarus, v. 380, p. 114965, doi:10.1016/j.icarus.2022.114965.
487 Carter, J., Loizeau, D., Mangold, N., Poulet, F., and Bibring, J., 2015, Widespread surface
488   weathering on early Mars : A case for a warmer and wetter climate: Icarus, v. 248, p.
489   373–382, doi:10.1016/j.icarus.2014.11.011.
490 Fernández, J.M., Peltre, C., Craine, J.M., and Plante, A.F., 2012, Improved characterization of
491   soil organic matter by thermal analysis using CO2/H2O evolved gas analysis:
492   Environmental Science and Technology, v. 46, p. 8921–8927, doi:10.1021/es301375d.
493 François, P., Szopa, C., Buch, A., Coll, P., Mcadam, A.C., Mahaffy, P.R., Freissinet, C., Glavin,
494   D.P., and Cabane, M., 2015, Magnesium sulfate as a key mineral for the detection of
495   organic molecules on Mars using pyrolysis: Journal of Geophysical Research – Planets,
496   p. 61–74, doi:10.1002/2015JE004884.Received.
497 Guggenberger, G., and Kaiser, K., 2003, Dissolved organic matter in soil : challenging the
498   paradigm of sorptive preservation: Geoderma, v. 113, p. 293–310, doi:10.1016/S0016-
499   7061(02)00366-X.
500 Hays, L.E., Graham, H. V., Des Marais, D.J., Hausrath, E.M., Horgan, B., McCollom, T.M.,
501   Parenteau, M.N., Potter-McIntyre, S.L., Williams, A.J., and Lynch, K.L., 2017,
502   Biosignature Preservation and Detection in Mars Analog Environments: Astrobiology,
503   v. 17, p. 363–400, doi:10.1089/ast.2016.1627.
504 Horgan, B., 2016, Strategies for Searching for Biosignatures in Ancient Martian Sub-Aerial
505   Surface Environments: Biosignature Preservation and Detection in Mars Analog
506   Environments, p. 7463, doi:10.1089/ast.2016.1627.
507 Ibarra, D.E., Egger, A.E., Weaver, K.L., Harris, C.R., and Maher, K., 2014, Rise and fall of late
508   Pleistocene pluvial lakes in response to reduced evaporation and precipitation:
509   Evidence from Lake Surprise, California: Bulletin of the Geological Society of America,
510   v. 126, p. 1387–1415, doi:10.1130/B31014.1.
511 Kleber, M., Bourg, I.C., Coward, E.K., Hansel, C.M., Myneni, S.C.B., and Nunan, N., 2021,
512   Dynamic interactions at the mineral–organic matter interface: Nature Reviews Earth
513   and Environment, v. 2, p. 402–421, doi:10.1038/s43017-021-00162-y.
514 Krull, E.S., and Retallack, G.J., 2000, 13C depth profiles from paleosols across the Permian-
515   Triassic boundary : Evidence for methane release: GSA Bulletin, v. 112, p. 1459–1472.
516 Lawrence, C.R., Harden, J.W., Xu, X., Schulz, M.S., and Trumbore, S.E., 2015, Long-term

517 controls on soil organic carbon with depth and time: A case study from the Cowlitz
518 River Chronosequence, WA USA: Geoderma, v. 247–248, p. 73–87,
519 doi:10.1016/j.geoderma.2015.02.005.
520 Liu, J., Michalski, J.R., Tan, W., He, H., Ye, B., and Xiao, L., 2021, Anoxic chemical weathering
521 under a reducing greenhouse on early Mars: Nature Astronomy,
522 doi:https://doi.org/10.1038/s41550-021-01303-5.
523 Marin-spiotta, E., Chaopricha, N.T., Plante, A.F., Diefendorf, A.F., Mueller, C.W., Grandy, A.S.,
524 and Mason, J.A., 2014, Long-term stabilization of deep soil carbon by fire and burial
525 during early Holocene climate change: Nature Geoscience, doi:10.1038/NGEO2169.
526 Marin-Spiotta, E., Chaopricha, N.T., Plante, A.F., Diefendorf, A.F., Mueller, C.W., Grandy, A.S.,
527 and Mason, J.A., 2014, Long-term stabilization of deep soil carbon by fire and burial
528 during early Holocene climate change: Nature Geoscience, v. 7, p. 428–432,
529 doi:10.1038/ngeo2169.
530 Matthewman, R., Cotton, L.J., Martins, Z., and Sephton, M.A., 2012, Organic geochemistry of
531 late Jurassic paleosols (Dirt Beds) of Dorset , UK: Marine and Petroleum Geology, v.
532 37, p. 41–52, doi:10.1016/j.marpetgeo.2012.05.009.
533 Mcadam, A.. et al., 2014, Sulfur-bearing phases detected by evolved gas analysis of the
534 Rocknest aeolian deposit, Gale Crater, Mars: Journal of Geophysical Research: Planets,
535 v. 119, p. 6121–6139, doi:10.1002/2013JE004518.Received.
536 Pataki, D.E., Ehleringer, J.R., Flanagan, L.B., Yakir, D., Bowling, D.R., Still, C.J., Buchmann, N.,
537 Kaplan, J.O., and Berry, J.A., 2003, The application and interpretation of Keeling plots in
538 terrestrial carbon cycle research: Global Biogeochemical Cycles, v. 17,
539 doi:10.1029/2001GB001850.
540 Plante, A.F., Fernández, J.M., Haddix, M.L., Steinweg, J.M., and Conant, R.T., 2011, Biological,
541 chemical and thermal indices of soil organic matter stability in four grassland soils: Soil
542 Biology and Biochemistry, v. 43, p. 1051–1058, doi:10.1016/j.soilbio.2011.01.024.
543 Raven, M.R., Fike, D.A., Gomes, M.L., Webb, S.M., Bradley, A.S., and Mcclelland, H.O., 2018,
544 Organic carbon burial during OAE2 driven by changes in the locus of organic matter
545 sulfurization: Nature Communications, v. 9, doi:10.1038/s41467-018-05943-6.
546 Retallack, G.J., Bestland, E.., and Fremd, T.., 2000, Eocene and Oligocene Paleosols of
547 Central Oregon: Geological Society of America Special Paper, v. 344, p. 1–192,
548 doi:10.1046/j.1365-3091.2001.0394c.x.
549 Retallack, G.J., Martin, J.E., Broz, A.P., Breithaupt, B.H., Matthews, A., and Walton, D.P., 2018,
550 Late Pleistocene mammoth trackway from Fossil Lake , Oregon: Paleogeography,
551 Paleoclimatology, Paleoecology, doi:10.1016/j.palaeo.2018.01.037.
552 Rye, R., and Holland, H., 2000, Life associated with a 2 . 76 Ga ephemeral pond ?: Evidence
553 from Mount Roe # 2 paleosol: Geology, v. 28, p. 483–486, doi:10.1130/0091-
554 7613(2000)28<483:LAWAGE>2.0.CO;2.
555 Sanderman, J., and Stuart Grandy, A., 2020, Ramped thermal analysis for isolating
556 biologically meaningful soil organic matter fractions with distinct residence times: Soil,
557 v. 6, p. 131–144, doi:10.5194/soil-6-131-2020.
558 Schmidt, M.W.I. et al., 2011, Persistence of soil organic matter as an ecosystem property:
559 Nature, doi:10.1038/nature10386.

560 Shi, Z., Allison, S.D., He, Y., Levine, P.A., Hoyt, A.M., Beem-Miller, J., Zhu, Q., Wieder, W.R.,
561   Trumbore, S., and Randerson, J.T., 2020, The age distribution of global soil carbon
562   inferred from radiocarbon measurements: Nature Geoscience, v. 13, p. 555–559,
563   doi:10.1038/s41561-020-0596-z.

564 Sickman, J.O., DiGiorgio, C.L., Davisson, M.L., Lucero, D.M., and Bergamaschi, B., 2010,
565   Identifying sources of dissolved organic carbon in agriculturally dominated rivers using
566   radiocarbon age dating: Sacramento-San Joaquin River Basin, California:
567   Biogeochemistry, v. 99, p. 79–96, doi:10.1007/s10533-009-9391-z.

568 Silva, L.C.R., Corrêa, R.S., Doane, T.A., Pereira, E.I.P., Horwath, W.R., Silva, L.C.R., Corrêa, R.S.,
569   Doane, T.A., and Pereira, E.I.P., 2013, Unprecedented carbon accumulation in mined
570   soils : the synergistic effect of resource input and plant species invasion: Ecological
571   Applications, v. 23, p. 1345–1356, doi:10.1890/12-1957.1.

572 Soulet, G., Hilton, R.G., Garnett, M.H., Roylands, T., Klotz, S., Croissant, T., Dellinger, M., and
573   Le Bouteiller, C., 2021, Temperature control on CO2 emissions from the weathering of
574   sedimentary rocks: Nature Geoscience, v. 14, p. 665–671, doi:10.1038/s41561-021-
575   00805-1.

576 Sutter, B., Mcadam, A.., Mahaffy, P.., Ming, D.., Edgett, K.., Rampe, E.., Eigenbrode, J.., Franz,
577   H.., and Freissinet, C., 2017, Evolved gas analyses of sedimentary rocks and eolian
578   sediment in Gale Crater, Mars: Results of the Curiosity rover's sample analysis at Mars
579   instrument from Yellowknife Bay to the Namib Dune: Journal of Geophysical Research :
580   Planets, p. 2574–2609, doi:10.1002/2016JE005225.

581 Sweeney, K.E., Roering, J.J., and Ellis, C., 2015, Experimental evidence for hillslope control of
582   landscape scale: Science, v. 349, p. 51–53, doi:10.1126/science.aab0017.

583 Trumbore, S., 2000, Age of Soil Organic Matter and Soil Respiration: Radiocarbon
584   Constraints on Belowground C Dynamics: Ecological Applications, v. 10, p. 399,
585   doi:10.2307/2641102.

586 Watanabe, Y., Martin, J.E.., and Ohmoto, H., 2000, Geochemical evidence for terrestrial
587   ecosystems 2.6 billion years ago: Nature, v. 408, doi:10.1038/35046052.

588 Watanabe, Y., Stewart, B.W., and Ohmoto, H., 2004, Organic- and carbonate-rich soil
589   formation ~2.6 billion years ago at Schagen, East Transvaal district, South Africa:
590   Geochimica et Cosmochimica Acta, v. 68, p. 2129–2151, doi:10.1016/j.gca.2003.10.036.

591 Williams, E.K., Fogel, M.L., Berhe, A.A., and Plante, A.F., 2018, Distinct bioenergetic
592   signatures in particulate versus mineral-associated soil organic matter: Geoderma, v.
593   330, p. 107–116, doi:10.1016/j.geoderma.2018.05.024.

594 Wright, J.L., Bomfim, B., Wong, C.I., Marimon-Júnior, B.H., Marimon, B.S., and Silva, L.C.R.,
595   2021, Sixteen hundred years of increasing tree cover prior to modern deforestation in
596   Southern Amazon and Central Brazilian savannas: Global Change Biology, v. 27, p.
597   136–150, doi:10.1111/gcb.15382.

598 Ye, B., and Michalski, J.R., 2021, Precipitation-Driven Pedogenic Weathering of
599   Volcaniclastics on Early Mars: Geophysical Research Letters, v. 48, p. 1–10,
600   doi:10.1029/2020GL091551.

601 Zech, M., Kreutzer, S., Zech, R., Goslar, T., Meszner, S., Mcintyre, C., Häggi, C., Eglinton, T.,
602   Faust, D., and Fuchs, M., 2017, Comparative 14C and OSL dating of loess-paleosol

603   sequences to evaluate post-depositional contamination of n-alkane biomarkers:

604   Quaternary Research, v. 87, p. 180–189, doi:10.1017/qua.2016.7.

605

606

607

608